

Effect of hot and cold deformation of a maraging steel C300 on the transformation kinetics from dilatometric curves.

Ricardo Vilain de Melo^{1*}, Carlos Augusto Silva de Oliveira²

^{1*}- Corresponding Author. Department of Mechanical Engineering, Universidade Federal de Santa Catarina, Rua Engenheiro Agrônomo Andrei Cristian Ferreira, s/n - Trindade, Florianópolis, Santa Catarina, Brazil.

²- Universidade Federal de Santa Catarina, Universidade Federal de Santa Catarina, Rua Engenheiro Agrônomo Andrei Cristian Ferreira, s/n - Trindade, Florianópolis, Santa Catarina, Brazil.

ABSTRACT

The modified Kissinger method was used to study the influence of deformation on the dilatometry curves of a high Ti maraging steel C300. Using heating rates between 0.083 and 0.333 K s⁻¹ it was possible to observe four distinct transformation regions characterized by recovery, recrystallization, precipitation and shear and diffusional austenite formation. When deformed, it was possible to observe that the cold deformation accelerated the transformations in the temperature between 603 and 770 K, while the hot deformation reduced the activation energy in the temperature between 743 and 870 K. When analyzing the temperature range that forms precipitates Ni₃Ti and Fe₂Mo, the activation energy in the hot, cold and non-deformed samples were 276, 175 and 242 kJmol⁻¹, respectively. Both deformations reduced the activation energy of the diffusion $\alpha' \rightarrow \gamma$ transformation from 456 kJmol⁻¹, in the non-deformation condition, to 304 and 365 kJmol⁻¹, in the hot and cold deformed samples, respectively.

KEYWORDS: dilatometry; maraging steel; precipitates; austenite; deformation; Kissinger method

Date of Submission: 18-06-2020

Date of acceptance: 06-07-2020

I. INTRODUCTION

Maraging steels are martensitic steels with low C and ultrahigh-strength hardened due to precipitation [1–3]. These steels have several applications ranging from the sports to the aerospace industry, and its most common use is in applications that require high strength and reliability, such as in the military and nuclear industries [1,4,5]. Commonly maraging steels are ferrous alloys containing Ni, Co, Mo and Ti, where the amount of these alloying elements will define their ultimate strength.

To achieve their final properties, these steels undergo two heat treatments: a solubilization, commonly performed at 1093 K, followed by aging at 753 K [4,6–9]. During the solubilization the maraging steels acquire a martensitic matrix supersaturated in alloy elements [10,11] containing a high density of dislocations [12]. During aging, the supersaturated alloying elements in the matrix diffuse into the crystalline defects, forming second phase particles which can be, at temperatures below 723 K, the phases S, X [13], ω [13–15], Ni₃(Ti, Mo) [14], for early times. For longer times, the phases Fe₂Mo and μ -Fe₇Mo₆ [15] start to form. When the maraging steel is aged at temperatures above 723 K, the A₃B type precipitation (A = Ni, Cr, Fe and B = Ti, Mo, Al) occurs due to the better interface coherence with the CCC matrix [10,12,16]. At longer aging times, Fe₂Mo and/or Fe₆Mo₇ follow its formation [10,15,17–20]. In even longer times, the formation of the reverse austenite can occur, due to the dissolution of A₃B precipitates and consequent local increase of Ni and Co content, austenite [17,21–24], as well as due to the segregation of these elements to the boundary of the martensite lath and grain boundary of the previous austenite [25].

The formation of new phases occur mainly by heterogeneous nucleation [26–28]. The growth, however, can be controlled both by pipe diffusion, due to the high dislocations density present in the martensitic matrix [10,29], and/or by lattice diffusion, when in higher heating rates [30] - since the activation energy obtained by several authors is close to the diffusion energy of Ti and Mo in a ferritic matrix [30–33]. The dominant hardening mechanism in maraging steels is Orowan and the main hardening phase of this steel is the metastable

Ni₃Ti, while the stable phase, Fe₂Mo and/or Fe₆Mo₇, has a lower contribution to hardening and it forms at higher aging times/temperatures[34].

The increase in the number of crystalline defects due to deformation tends to accelerate the kinetics of heterogeneous precipitation [35]. This agreed with the acceleration of Ni₃Ti precipitation kinetics in cold deformed samples found by Lian et al [36]. However, although there is an initial increase in hardness, a hot deformation process delays the kinetics of precipitation [37].

This deformation also affects the formation of reverse austenite. As it preferentially occurs in the boundary of the martensite lath [6], the refining of this structure resulting from the hot deformation [37] accelerate the kinetics of austenite formation. In the same way, the deformation promotes a finer precipitation, which later dissolves and enrich the matrix locally with Ni, accelerating the kinetics of austenite formation [6]. Although the reverse austenite decrease the mechanical strength, its presence may be beneficial in cases where there is a need for greater toughness [31].

There are several studies correlating precipitation and austenite transformation temperature with dilatometric curves. These studies, using the modified Kissinger method described by the equation 1, estimated the activation energy in transformations for distinct classes of maraging steels [1,30,32–34,38–41].

$$\ln(\varphi^2/Tm) = -E/(R \times Tm) + C \quad \text{Eq. 1}$$

Where φ is the heating rate, Tm is the maximum transformation temperature for the given heating rate, E is the activation energy, R is the universal gas constant and C is a constant.

However, the effect of deformation on the activation energy[37] and phase fraction transformed into maraging steels is little studied[24,27,38,39,42,43]. Therefore, this study aims to fill this gap by verifying the influence of hot and cold deformation on the transformation temperatures and precipitation kinetics of a high-Ti C300 maraging steel.

II. MATERIALS AND METHODS

The studied material, given in Table 1, was provided in the form of two 140 mm diameter discs, each with 10 and 20 mm thick. From the 10 mm thick disc, eight cubic samples with 10 mm of edge were removed and solubilized at 1323 K for 1 h. After solubilization, four samples were cooled in water, while the remaining samples were hot forged at 1323 K with 50% reduction in height in single pass and then cooled in water. The 20 mm thick disk was initially cut in a rectangular format of 100 x 50 x 20 mm and then rolled in two ways: the first with a 50% height reduction at a temperature of 1473 K cooled in water, and the second also with a 50% height reduction at room temperature. The three study conditions were obtained: No deformation (0%), hot forging (F50%) and hot and cold rolled (R50%50%).

From each study condition, four rectangular samples of dimensions 10 x 5 x 5 mm were machined from the central region of the samples. Then these samples were analyzed by dilatometry on a Netzch 402C dilatometer in the temperature range of 373 to 1173 K with heating rates of 0.0833, 0.166, 0.250 and 0.333 K s⁻¹.

Table 1: Chemical composition of the studied material in wt%.

Ni	Co	Mo	Ti	Al	C	Mn	Si	Fe
18.6	9.4	5.2	1.0	0.10	0.03	0.04	0.19	Bal

III. RESULTS AND DISCUSSION

Figure 1 shows the dilatometric curves for the conditions 0%, F50% and R50%50% at heating rate of 0.166 K s⁻¹. The loss of linearity of a dilatometric curve indicates the occurrence of an atomic rearrangement, which in maraging steels may be associated with: recovery of the martensite[22], formation of carbides [22] and precipitates, diffusional and/or shear $\alpha' \rightarrow \gamma$ transformation[32,38] and recrystallization of the microstructure[44]. During the cooling, the loss of linearity indicates a $\gamma \rightarrow \alpha'$ transformation [45].

Figure 2 shows the curve $d(l/l_0)/dt$ as a function of temperature for a heating rate of 0.166 K s⁻¹, where four distinct transformation regions are visible: T1, T2, T3 and T4. The start and end of each of the transformations were obtained from the curve $d^2(l/l_0)/dT^2$ as a function of temperature, and are given in table 2. The suffix s and f in table 2 indicates the initial and final temperature, respectively.

Region T1 (~600-750 K) is characterized by the recovery of the martensitic structure and the formation of carbides [22] and low temperature precipitates of the ω type [18], which, due to the absence of incubation time, may form even with high heating rates [46]. Region T2 (~750-850 K) is characterized by the formation of the meta stable phase A₃B and the stable Fe₂Mo and/or Fe₇Mo₆[10,12,16,18–20,47,48]. These phases always form after precipitation of ω phase [11]. Region T3 (~850-1000 K) is characterized as a result of the diffusional reverse austenite formation while Region T4 (~1000-1050 K) is characterized by the reverse austenite transformation by shear[3,16,19,38,39].

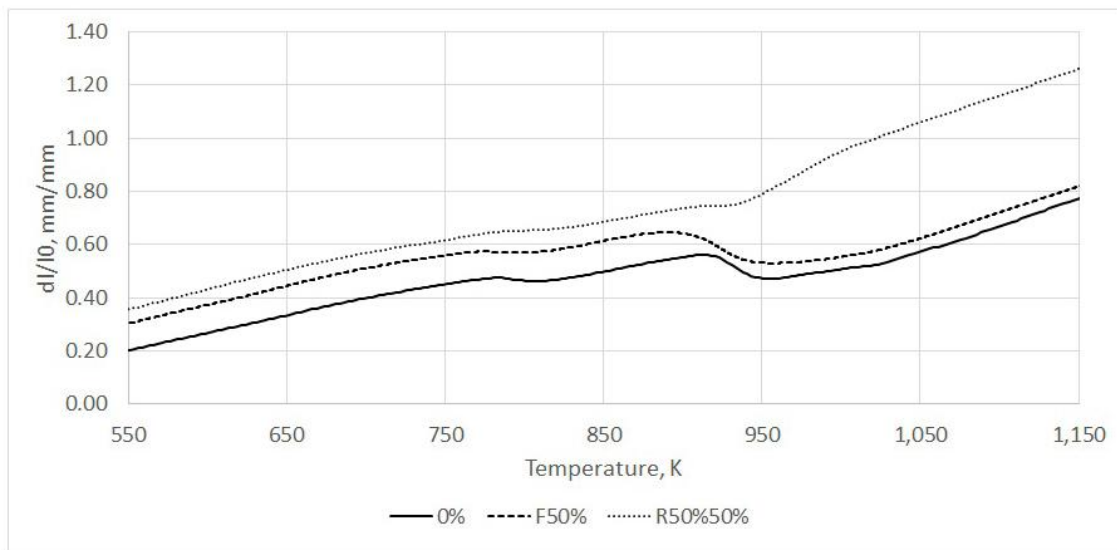


Fig. 1 Dilatometric curves for the conditions 0%, F50% and R50%50% heated at 0.166 k s^{-1}

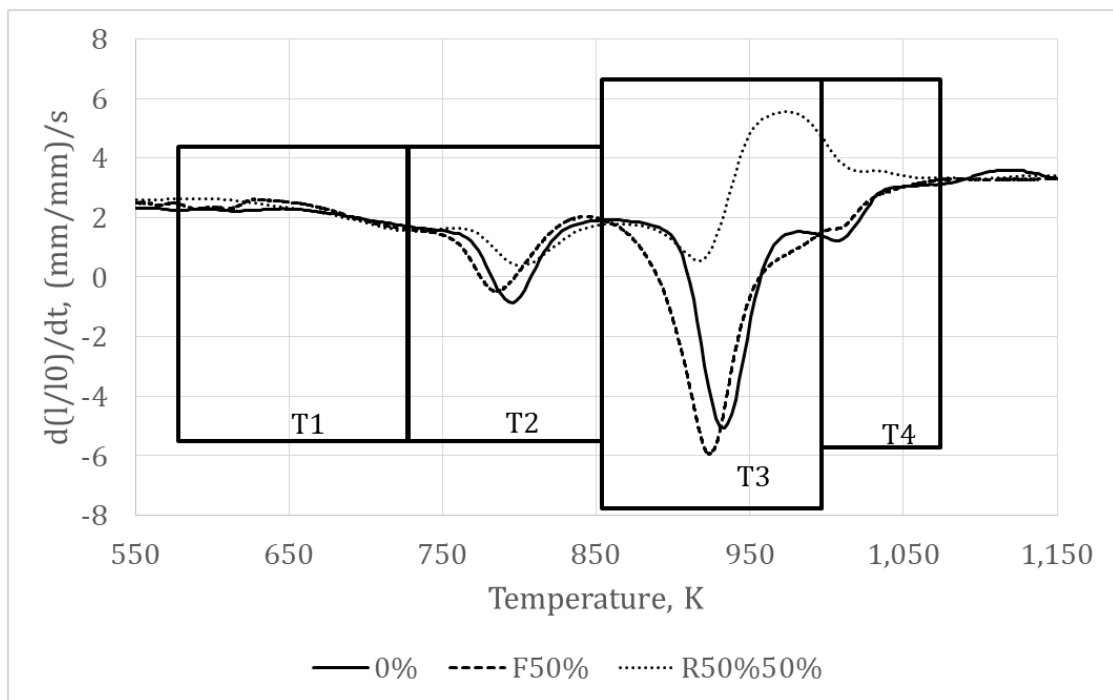


Fig. 2: Plot of $d(l/l_0)/dt$ for the conditions 0%, F50% and R50%50% heated at 0.166 K s^{-1}

Table 2: Start and final temperatures for all conditions analyzed.

Deformation	Heating Hate, K s^{-1}	Temperature, K							
		T1s	T1f	T2s	T2f	T3s	T3f	T4s	T4f
0%	0.083	633	708	711	841	863	976	978	1038
	0.166	646	763	766	853	871	981	983	1038
	0.250	633	768	771	851	893	988	991	1038
	0.333	671	771	773	866	883	991	993	1041
F50%	0.083	627	733	734	828	829	979	980	1079
	0.166	633	740	741	845	846	986	987	1071
	0.250	682	759	759	851	860	1010	1010	1064

	0.333	676	766	766	860	870	1021	1021	1081
L50%50%	0.083	633	741	743	838	871	946	948	1066
	0.166	603	761	763	858	871	973	976	1066
	0.250	616	763	766	871	873	976	978	1078
	0.333	616	771	773	871	873	976	978	1078

Activation Energy and Dilatation

Table 3 contains the value of T_m for regions T1, T2, T3, obtained from the minimum values given by graph $d(l/l_0)/dt$ versus temperature. Region T1 in the 0% and F50% conditions did not present a minimum value, therefore it was not possible to obtain the value of T_m in this condition.

Figure 3 shows the trend lines for the values of T2 in the conditions 0%, F50% and R50%50% calculated from equation 1 with data obtained in Table 3. The angular coefficient of the trend lines represents the activation energy, E, provided in Table 4 for each analyzed condition besides some values found in literature. Although the values of T_m could be observed in region T4, it did not present a linear response when plotted on the graph $\ln(\phi^2/T_m)$ as a function of $1/(RT_m)$, making it difficult to estimate E with the modified Kissinger method.

This happened because a premise of the Kissinger method is that, in order to obtain different values of T_m , the transformation must be dependent on the heating rate, in other words, controlled by diffusion, which does not occur with shear like transformations, such as occurs in region T4. For a diffusional transformation take place, it need time to reach the required composition, but as higher is the heat rate, the shorter is the time available for transformation at a certain temperature, that make the transformation take place at higher temperatures.

It is believed that for these reasons the distinction between regions T1 and T2, or T3 and T4, was not observed in literature, and the estimated value of E for precipitation consists on the obtained values for region T2, while this value for the $\alpha' \rightarrow \gamma$ transformation is estimated by the diffusional $\alpha' \rightarrow \gamma$ transformation, T3 region.

The obtained value of E for region T2 in the 0% condition was 242 kJ mol^{-1} . This is in agreement with values observed in the literature, Table 4, and is close to the values of E for the diffusion of Ti, Mo and Ni in iron α , 293 [49], 282 [50] and 245 kJ mol^{-1} [51], respectively. This indicates the occurrence of a diffusional transformation with those three elements, probably the precipitation of Ni_3Ti , Fe_2Mo and/or Fe_7Mo_6 , and the slightly reduction of E occurred due to the high density of dislocations present in the martensitic matrix.

To understand the effects of deformation on the transformations, it is important to analyze the total dilatation for all regions: ΔT_1 , ΔT_2 , ΔT_3 and ΔT_4 . For this, the values of ΔT_x were calculated as shown in Figure 4 and the mean value of these results is shown in table 5. Analyzing the values of ΔT_1 it is possible to verify that the cold deformation increased the transformed volume in region T1 due to the heterogeneous nucleation promoted by the number of crystalline defects [35], while no changes could be seen from the cold deformation.

Alongside the increase of transformed volume in region T1, the recovery of the microstructure caused a reduction in the number of dislocations. Add to this, an impoverishment of alloying elements in the matrix occurs due to the precipitation of the S and ω phase. Those two factors lead to a reduction in the driving force for subsequent T2 transformations and, consequently, a greater E value for region T2 in the cold deformed samples when compared to non-deformed ones.

The opposite happens with the hot-deformed sample, where occurs a significant reduction of E in the region T2. It probably happens due the austenite recrystallization that occurs while the samples are deformed. The resulting amount of dislocation from this process is not enough to promote the transformations in region T1, but enables a higher quantity of heterogeneous precipitations in region T2.

The value of ΔT_2 decrease when a deformation is applied, independent if the activation energy increased or decreased. That occurs due to the higher amount of dislocations in the deformed samples. Once the misfit between matrix and precipitate is minimized on a crystalline defect as dislocation and grains boundary, a precipitation in those defects tends to minimize the dilatation caused by them [35].

Lian et al [36], when cold rolling the material, did not find a reduction in volume of Ni_3Ti in the region T2. That has occurred, probably, because Lian et al only analyzed samples aged at 783 K, where the rapid heating of the samples inhibited the precipitation of X, S and ω , causing the high density of dislocation to aid the heterogeneous precipitation of Ni_3Ti .

The value of E for region T3, characterized by diffusional $\alpha' \rightarrow \gamma$ transformation, is strongly influenced by the heating rate, ranging from 423 kJ mol^{-1} , for rates lower than 2 K s^{-1} , to 828 kJ mol^{-1} , for rates higher than 2 K s^{-1} in a non-deformed sample [33]. In this work, the value found, for the T3 region in the 0% condition and heating rates below 0.333 K s^{-1} , were 456 kJ mol^{-1} , falling dramatically when applied a deformation, reaching

304 and 365 kJ mol⁻¹, under the conditions F50% and L50%50%, respectively. This fall occurs due to the previous transformations that took place in regions T1 and T2. That happens because the deformation not only accelerates the formation of S, ω and Ni₃Ti precipitates, but their dissolution as well, as they are metastable phases. That dissolution enriches the matrix with Ni and Co that leads to an increase on the driving force of α'→γ transformation and, consequently, a decrease in the value of E, as verified.

Although the reduction of the E value in region T3 indicates an increase in the diffusional α'→γ transformation due to deformation, that could only be seen only on the hot deformed samples. In the cold deformed, the created texture prevented a direct comparison between the dilatations in this region. This occurs because the texture generates a preferential direction for the α'→γ transformation distinct for the three conditions of analysis[40].

Table 3: Maximum transformation temperatures, T_m, for all conditions studied.

Deformation	Heating Rate, K s ⁻¹	Temperature, K		
		T1	T2	T3
0%	0.083	-	783	923
	0.166	-	796	933
	0.250	-	806	941
	0.333	-	811	943
F50%	0.083	-	774	915
	0.166	-	785	924
	0.250	-	801	938
	0.333	-	809	943
R50%50%	0.083	713	788	906
	0.166	733	801	918
	0.250	741	808	926
	0.333	743	813	931

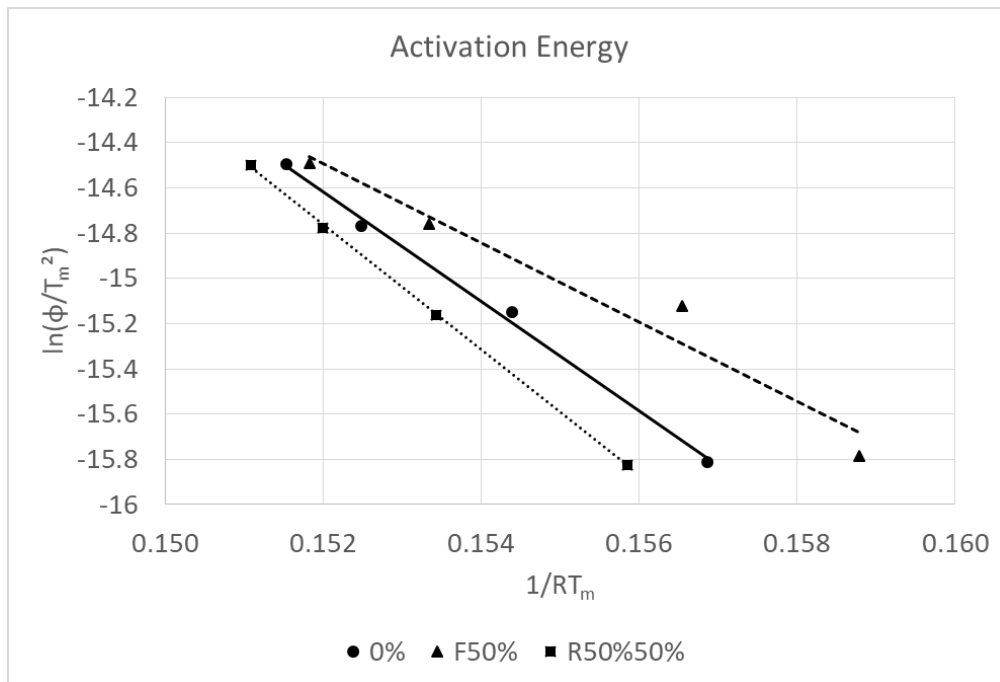


Fig. 3 Plot of the trend lines from the points calculated by equation 1 for the transformation in region 2

Table 4: Activation energy obtained in this work and verified in the literature.

Region	Activation Energy (kJ mol ⁻¹)			Reference	Maraging
	0%	F50%	L50%50%		
T1	-	-	175	This Work	C300
T2	242	175	276	This Work	C300
	205	-	-	[31]	C250
	145	-	-	[32]	C300
	265	-	-	[33]	C350
	272	-	-	[30]	C300
	276	-	-	[30]	C350
T3	456	304	365	This Work	C300
	342	-	-	[31]	C250
	224	-	-	[32]	C300
	423($\phi < 2$) e 828($\phi > 2$)	-	-	[33]	C350
	562	-	-	[30]	C300
	569/642	-	-	[30]	C350

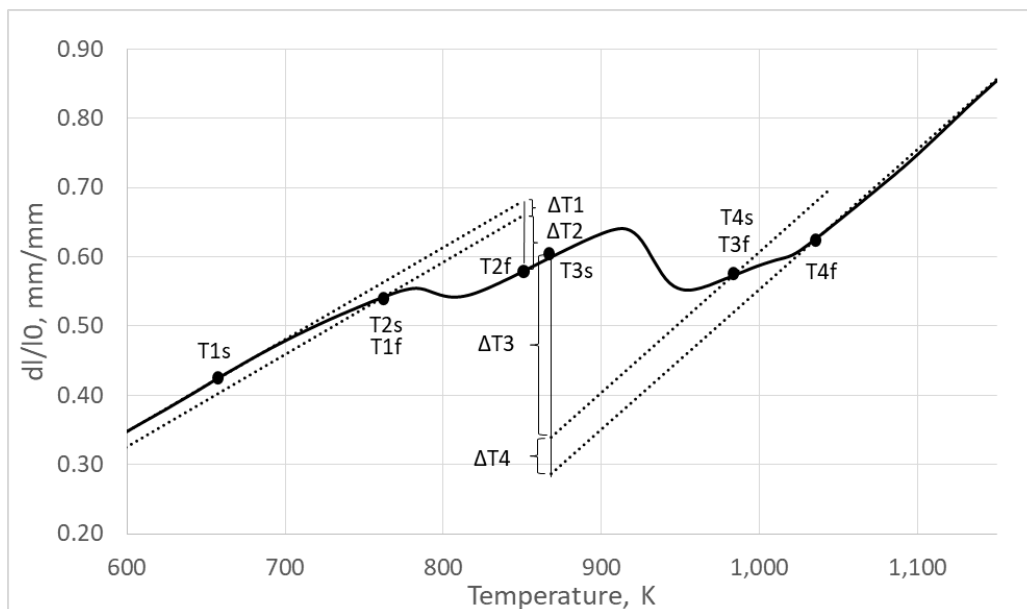


Fig. 4 Sketch of how the calculation of $\Delta T1$, $\Delta T2$, $\Delta T3$ and $\Delta T4$ was performed for the 0% condition heated to 0.166 K s^{-1}

Table 5: Mean values of $\Delta T1$, $\Delta T2$, $\Delta T3$ and $\Delta T4$ for all study conditions.

Deformation	$\Delta T1$, mm/mm	$\Delta T2$, mm/mm	$\Delta T3$, mm/mm	$\Delta T4$, mm/mm
0%	0.0222	0.0992	0.2440	0.0488
F50%	0.0222	0.0871	0.2992	0.0320
R50%50%	0.0370	0.0792	-0.0020	0.0500

IV. CONCLUSION

It is possible to conclude from the experimental data that the cold deformation improved the transformation kinetics in region T1 that was characterized by an increase of the total contraction, ΔT_1 . The cold deformation also made it possible to calculate the activation energy, E , for the region T1, 175 kJ mol^{-1} . In region T2, the calculated value of E for non-deformed samples was 242 kJ mol^{-1} . The cold and hot deformation seems to have affected differently the kinetics of the transformation - hot deformation decreased the value of E to 175 kJ mol^{-1} , while cold deformation increased it to 276 kJ mol^{-1} .

Probably those changes in the activation energy occurred due to the increase in the number of dislocations resulting from the deformation, leading to a greater heterogeneous nucleation of precipitates.

The deformation also reduced the activation energy of the diffusional $\alpha' \rightarrow \gamma$ transformation, region T3, from 456 kJ mol^{-1} , for the condition 0%, to 304 and 365 kJ mol^{-1} , for the conditions F50% and R5050%, respectively. This probably occurred because the deformation not only accelerates the precipitation of S, ω and Ni_3Ti , but also their dissolution, that leads to a locally enrichment of the matrix with Ni and Mo, increasing the driving force for the diffusional $\alpha' \rightarrow \gamma$ transformation.

ACKNOWLEDGMENT

The authors want to acknowledge the CAPES and CNPq for the scholarship and the research grant that allowed the execution of this study.

Funding: This study was funded by CNPq (MCTIC/CNPq N° 28/2018 - Universal/Faixa B - 405133/2018-9 and CNPq N° 12/2017 - Bolsas de Produtividade em Pesquisa - PQ) and CAPES (Programa Pró defesa IV - Edital no 27/2018 CAPES)

Conflict of Interest: The authors declare that they have no conflict of interest.

REFERENCES

- [1]. W. Sha, Q. Li, E.A. Wilson, Precipitation, microstructure and mechanical properties of low nickel maraging steel, *Mater. Sci. Technol.* 27 (2011) 983–989. doi:10.1179/1743284710Y.0000000019.
- [2]. Y. He, K. Yang, W. Sha, Z. Guo, K. Liu, Age hardening and mechanical properties of a 2400 MPa grade cobalt-free maraging steel, *Metall. Mater. Trans. A Phys. Metall. Mater. Sci.* 37 (2006) 1107–1116. doi:10.1007/s11661-006-1089-4.
- [3]. R. Casati, J. Lemke, A. Tuissi, M. Vedani, Aging Behaviour and Mechanical Performance of 18-Ni 300 Steel Processed by Selective Laser Melting, *Metals (Basel)*. 6 (2016) 1–13. doi:10.3390/met6090218.
- [4]. W. Sha, Z. Guo, *Maraging Steels: Modelling of Microstructure, Properties and Applications*, 1st ed., Woodhead Publishing, Oxford, 2009.
- [5]. A.M. Hall, C.J. Slunder, *The Metallurgy, Behavior, and Application of the 18-Percent Bickel Maraging Steels*, Washington, D.C., 1968.
- [6]. A. Ali, M. Ahmed, F.H. Hashmi, A.Q. Khan, Austenite reversion in cold formed 18 wt-%Ni 350 grade maraging steel, *Mater. Sci. Technol.* 10 (1994) 97–101. doi:10.1179/mst.1994.10.2.97.
- [7]. R. Kapoor, S. Sunil, G. Bharat Reddy, S. Nagaraju, T.S. Kolge, S.K. Sarkar, Sarita, A. Biswas, A. Sharma, Electric current induced precipitation in maraging steel, *Scr. Mater.* 154 (2018) 16–19. doi:10.1016/j.scriptamat.2018.05.013.
- [8]. C.N. Park, Y.G. Kim, Effects of repeated thermal cyclings on the transformation behaviour, microstructure and mechanical properties in a cobalt-free tungsten-containing maraging steel (W-250), *Mater. Sci. Eng. A.* 123 (1990) 255–260. doi:10.1016/0921-5093(90)90291-A.
- [9]. F. Cajner, D. Landek, S. Šolić, H. Cajner, Effects of thermochemical treatments on properties of maraging steels, *Surf. Eng.* 22 (2006) 468–471. doi:10.1179/174329406x150486.
- [10]. V.K. Vasudevan, S.J. Kim, C.M. Wayman, Precipitation reactions and strengthening behavior in 18 Wt Pct nickel maraging steels, *Metall. Trans. A, Phys. Metall. Mater. Sci.* 21 A (1990) 2655–2668. doi:10.1007/BF02646061.
- [11]. W. Sha, A. Cerezo, G. Smith, Phase chemistry and precipitation reactions in maraging steels: Part IV. Discussion and conclusions, *Metall. Trans. A.* 24 (1993) 1251–1256. doi:10.1007/BF02668193.
- [12]. K. Macek, P. Lukáš, J. Janovec, P. Mikula, P. Strunz, M. Vrána, M. Zaffagnini, Austenite content and dislocation density in electron-beam welds of a stainless maraging steel, *Mater. Sci. Eng. A.* 208 (1996) 131–138. doi:10.1016/0921-5093(95)10047-4.
- [13]. R. Tewari, S. Mazumder, I.S. Batra, G.K. Dey, S. Banerjee, Precipitation in 18 wt% Ni maraging steel of grade 350, *Acta Mater.* 48 (2000) 1187–1200. doi:10.1016/S1359-6454(99)00370-5.
- [14]. J.M. Pardo, S.S.M. Tavares, M.P. Cindra Fonseca, H.F.G. Abreu, J.J.M. Silva, Study of the austenite quantification by X-ray diffraction in the 18Ni-Co-Mo-Ti maraging 300 steel, *J. Mater. Sci.* 41 (2006) 2301–2307. doi:10.1007/s10853-006-7170-y.
- [15]. W. Sha, A. Cerezo, G.D.W. Smith, Phase chemistry and precipitation reactions in maraging steels: Part III. Model Alloys, *Metall. Mater. Trans. A.* 24 (1993) 1241–1249. doi:10.1007/BF02668192.
- [16]. S. Floreen, *The Physical Metallurgy of Maraging Steels*, *Metall. Rev.* (1968) 115–128. doi:10.1179/mtr.1968.13.1.115.
- [17]. M. Ahmed, I. Nasim, S.W. Husain, Influence of nickel and molybdenum on the phase stability and mechanical properties of maraging steels, *J. Mater. Eng. Perform.* 3 (1994) 248–254. doi:10.1007/BF02645850.
- [18]. J.B. Lecomte, C. Servant, G. Cizeron, A comparison of the structural evolution occurring during anisothermal or isothermal treatments in the case of nickel and manganese type maraging alloys, *J. Mater. Sci.* 20 (1985) 3339–3352. doi:10.1007/BF00545204.
- [19]. K. Rohrbach, M. Schmidt, *ASM Handbook, Volume 1: Properties and Selection: Irons, Steels, and High-Performance Alloys*, ASM International, 1990. doi:10.1361/asmhba0001043.
- [20]. K. Stiller, F. Danoix, A. Bostel, Investigation of precipitation in a new maraging stainless steel, *Appl. Surf. Sci.* 94–95 (1996) 326–333. doi:10.1016/0169-4332(95)00394-0.
- [21]. Y. He, K. Yang, W. Sha, Microstructure and Mechanical Properties of a 2000 MPa Grade Co-Free Maraging Steel, *Metall. Mater. Trans. A Phys. Metall. Mater. Sci.* 36 A (2005) 2273–2287. doi:10.1007/s11661-005-0100-9.

- [22]. D.T. Peters, C.R. Cupp, The Kinetics of Aging Reactions in 18 Pct Ni Maraging Steels, *Trans. Metall. Soc. AIME*. 236 (1966) 1420–1429.
- [23]. X. Li, Z. Yin, Reverted austenite during aging in 18Ni(350) maraging steel, *Mater. Lett.* 24 (1995) 239–242. doi:10.1016/0167-577X(95)00109-3.
- [24]. S.S.M. Tavares, H.F.G. Abreu, J.M. Neto, M.R. da Silva, I. Popa, A thermomagnetic study of the martensite–austenite phase transition in the maraging 350 steel, *J. Alloys Compd.* 358 (2003) 152–156. doi:10.1016/S0925-8388(03)00335-9.
- [25]. U.K. Viswanathan, G.K. Dey, V. Sethumadhavan, Effects of austenite reversion during overaging on the mechanical properties of 18 Ni (350) maraging steel, *Mater. Sci. Eng. A*. 398 (2005) 367–372. doi:10.1016/j.msea.2005.03.074.
- [26]. J.M. Oblak, W.A. Owczarski, B.H. Kear, HETEROGENEOUS PRECIPITATION OF METASTABLE BASE ALLOY, *Acta Metall.* 19 (1971) 355–363. doi:10.1016/0001-6160(71)90103-9.
- [27]. A. Shekhter, M.K. Miller, H.I. Aaronson, E. V. Pereloma, S.P. Ringer, Effect of aging and deformation on the microstructure and properties of Fe–Ni–Ti maraging steel, *Metall. Mater. Trans. A*. 35 (2004) 973–983. doi:10.1007/s11661-004-1001-z.
- [28]. M. Nili Ahmadabadi, H. Shirazi, H. Ghasemi-Nanesa, S. Hossein Nedjad, B. Poorganji, T. Furuahara, Role of severe plastic deformation on the formation of nanograins and nano-sized precipitates in Fe-Ni-Mn steel, *Mater. Des.* 32 (2011) 3526–3531. doi:10.1016/j.matdes.2011.02.018.
- [29]. C. Servant, P. Lacombe, Structural transformations produced during tempering of Fe-Ni-Co-Mo alloys, *J. Mater. Sci.* 12 (1977) 1807–1826. doi:10.1007/BF00566241.
- [30]. L.G. de Carvalho, M.S. Andrade, R.L. Plaut, F.M. Souza, A.F. Padilha, A dilatometric study of the phase transformations in 300 and 350 maraging steels during continuous heating rates, *Mater. Res.* 16 (2013) 740–744. doi:10.1590/s1516-14392013005000069.
- [31]. Z. Guo, W. Sha, D. Li, Quantification of phase transformation kinetics of 18 wt.% Ni C250 maraging steel, *Mater. Sci. Eng. A*. 373 (2004) 10–20. doi:10.1016/j.msea.2004.01.040.
- [32]. U.K. Viswanathan, T.R.G. Kutty, C. Ganguly, Dilatometric technique for evaluation of the kinetics of solid-state transformation of maraging steel, *Metall. Trans. A*. 24 (1993) 2653–2656. doi:10.1007/BF02659489.
- [33]. R. Kapoor, I.S. Batra, On the α' to γ transformation in maraging (grade 350), PH 13-8 Mo and 17-4 PH steels, *Mater. Sci. Eng. A*. 371 (2004) 324–334. doi:10.1016/j.msea.2003.12.023.
- [34]. F. Zhu, Y.F. Yin, R.G. Faulkner, Microstructural control of maraging steel C300, *Mater. Sci. Technol.* 27 (2011) 395–405. doi:10.1179/026708309X12506933873503.
- [35]. D. a. Porter, K.E. Easterling, *Phase Transformations in Metals and Alloys*, 2nd ed., CHAPMAN & HALL, London, 1992.
- [36]. Y. Lian, J. Huang, J. Zhang, C. Zhao, W. Gao, Z. Zhang, M. Ma, Effects of cold rolling on the microstructure and properties of Fe-Cr-Ni-Mo-Ti maraging steel, *Mater. Sci. Eng. A*. 712 (2018) 663–670. doi:10.1016/j.msea.2017.12.041.
- [37]. G.M.C. Güiza, C.A.S. Oliveira, Microstructural changes produced by hot forging in a C300 Maraging Steel, *Mater. Sci. Eng. A*. 655 (2016) 142–151. doi:10.1016/j.msea.2015.12.084.
- [38]. R. Kapoor, L. Kumar, I. Batra, A dilatometric study of the continuous heating transformations in 18wt.% Ni maraging steel of grade 350, *Mater. Sci. Eng. A*. 352 (2003) 318–324. doi:10.1016/S0921-5093(02)00934-6.
- [39]. U.K. Viswanathan, G.K. Dey, M.K. Asundi, Precipitation hardening in 350 grade maraging steel, *Metall. Trans. A*. 24 (1993) 2429–2442. doi:10.1007/BF02646522.
- [40]. M. Farooque, S. Qaisar, A.Q. Khan, A. Ul Haq, Dimensional anisotropy in 18 pct Ni maraging steel, *Metall. Mater. Trans. A Phys. Metall. Mater. Sci.* 32 (2001) 1057–1061. doi:10.1007/s11661-001-0116-8.
- [41]. A. Goldberg, D.G. O'Connor, Influence of heating rate on transformations in an 18 per cent nickel maraging steel, *Nature*. 213 (1967) 170–171. doi:10.1038/213170a0.
- [42]. G.H. de O. Freitas, C.A.S. de Oliveira, Effect of Hot Deformation on Microstructure, Hardness and Precipitation Kinetics in a C350 Maraging Steel Modified by Titanium Addition, *Mater. Res.* 21 (2018). doi:10.1590/1980-5373-mr-2018-0120.
- [43]. H.F.G. Abreu, S.S.M. Tavares, J.J.M. Silva, J.W.A. Menezes, A.D. Bruno, The influence of an intermediate austenitization heat treatment in the texture of cold-rolled and aged 18% Ni maraging steel, *Mater. Charact.* 52 (2004) 203–207. doi:10.1016/j.matchar.2004.05.007.
- [44]. G. Saul, J.A. Roberson, A.M. Adair, The Effects of Thermal Treatment on the Austenitic Grain Size and Mechanical Properties of 18 Pct Ni Maraging Steels, *Metall. Trans.* 1 (1970) 383–387. doi:10.1007/BF02811546.
- [45]. Y. He, K. Yang, W. Qu, F. Kong, G. Su, Strengthening and toughening of a 2800-MPa grade maraging steel, *Mater. Lett.* 56 (2002) 763–769. doi:10.1016/S0167-577X(02)00610-9.
- [46]. J.M. Pardal, S.S.M. Tavares, V.F. Terra, M.R. Da Silva, D.R. Dos Santos, Modeling of precipitation hardening during the aging and overaging of 18Ni–Co–Mo–Ti maraging 300 steel, *J. Alloys Compd.* 393 (2005) 109–113. doi:10.1016/j.jallcom.2004.09.049.
- [47]. W. Sha, A. Cerezo, G.D.W. Smith, Phase Chemistry and Precipitation Reactions in Maraging Steels" Part I. Introduction and Study of Co-Containing C-300 Steel, *Metall. Trans. A*. 24 (1993) 1221–1232. doi:10.1007/BF02668190.
- [48]. C. Tan, K. Zhou, W. Ma, P. Zhang, M. Liu, T. Kuang, Microstructural evolution, nanoprecipitation behavior and mechanical properties of selective laser melted high-performance grade 300 maraging steel, *Mater. Des.* 134 (2017) 23–34. doi:10.1016/j.matdes.2017.08.026.
- [49]. P. Klugkist, C. Herzig, Tracer diffusion of titanium in α -iron, 1995. doi:10.1002/pssa.2211480209.
- [50]. H. Nitta, T. Yamamoto, R. Kanno, K. Takasawa, T. Iida, Y. Yamazaki, S. Ogu, Y. Iijima, Diffusion of molybdenum in α -iron, *Acta Mater.* 50 (2002) 4117–4125. doi:10.1016/s1359-6454(02)00229-x.
- [51]. K. Hirano, M. Cohen, B.L. Averbach, Diffusion of Nickel into Iron, *Acta Metall.* 9 (1961) 440–445. doi:10.1016/0001-6160(61)90138-9.

Ricardo Vilain de Melo, et. al. "Effect of hot and cold deformation of a maraging steel C300 on the transformation kinetics from dilatometric curves." *American Journal of Engineering Research (AJER)*, vol. 9(07), 2020, pp. 09-16.